Analyzing Multitemporal Datasets to Monitor Topographic Changes in Rio Cucco Italy

Jad Ghantous[a], Vincenzo Di Pietra[b], Elena Belcore[c] and Nives Grasso[d]

DIATI, Politecnico di Torino, C.so Duca Degli Abruzzi, Turin, Italy

Keywords: Natural Hazards, Digital Terrain Model, Point Cloud, Semantic Segmentation, Deep Learning.

Abstract: Rio Cucco is an Italian catchment located in Malborghetto of Friuli Venezia Giulia. It is considered an area of interest regarding its hydrological and morphological properties. The area has historically been affected by natural hazards such as rockfall and landslides, mainly related to extreme rainfall events like the 2003 storm that affected the Fella river or the Vaia storm of October 2018. These events highlight the importance of understanding the morphological and topographic modification of the area also in relation to the realization of protection and hydraulic works. The changes in Rio Cucco were documented by comparing open-source historical data with ad-hoc UAV surveys focusing the analysis on 3D products like point clouds and the digital terrain models. The source of the recent data was an Aerial LiDAR- based survey conducted by our team in June 2024 while the historical data was taken from the FVG region's geoportal and referred to 2017. After comparing the different datasets with traditional techniques like nearest neighbour Euclidean distance or DEM of Difference, changes were evident pointing to potential rockfalls between the year 2024 and 2017. A deep learning model was explored and in development for the semantic segmentation of the area.

1 INTRODUCTION

Natural hazards are influenced by climatic conditions. Climate change affects the frequency and intensity of hazards such as landslides by modifying the hydrological regimes (Schneiderbauer et al., 2021). In a recent study by Semnani et al. (2025), landslide susceptibility was modeled across California based on different climate scenarios. They found that there was an overall increase in susceptibility in respect to time until the year 2100 in areas such as Sierra Nevada and the areas near the coast of California. Several areas have experienced landslides over the years. A landslide in Mount Meager Canada occurred in 2010 triggered by three decades of temperature increases that degraded the permafrost (Huggel et al., 2012). In the case of Italy, Monte Rosa was affected by a landslide in 2007 as a result of permafrost degradation as well (Huggel et al., 2012). Another example, is the Esino River basin in central Italy which was studied based on the relationship between climate change and

landslides (Sangelantoni et al., 2018). The frequent landslides prompted the creation of several research projects to study and monitor the relationship between the areas at risk of natural hazards and their geomorphological properties. Among these projects, PRIN funded MORPHEUS (GeoMORPHomEtry through Scales for a resilient landscape), which this case study was part of, aims to involve several research bodies to collaborate on the relationship between natural hazards and the sediment connectivity of the area. Sediment connectivity refers to the degree of linkage that controls sediment fluxes through a landscape, especially between the sediment source and the downstream area (Cavalli et al., 2013) Sediment connectivity is especially important in mountainous catchments. The presence of natural and anthropic structures (roads, terraces, dams) greatly affects the connectivity pathways. This as a result impacts the estimation of natural hazards. Therefore, morphological variations derived from multi-temporal topographic information are fundamental to

[a] https://orcid.org/ 0009-0001-3817-3578
[b] https://orcid.org/ 0000-0001-7501-1183
[c] https://orcid.org/ 0000-0002-3592-9384
[d] https://orcid.org/0000-0002-9548-6765

103

implement functional sediment connectivity analysis. In this context, a UAV survey represents the main source of high temporal resolution topographic data allowing the generation of several 3D products from LiDAR or Photogrammetric processing. Among these products, Digital Elevation Models are fundamental to derive structural connectivity parameters while DEMs of Difference are used to estimate the impact of topographic changes. Therefore, a multi-temporal analysis is crucial to successfully achieve the goal of the Morpheus project. In the case of this project, the regions particularly studied in the framework of sediment connectivity include Liguria, Veneto and Friuli Venezia Giulia. The selected study areas encompass several catchments located in contrasting landscapes of northern Italy and featuring different sediment transport processes. Among the many, Rio Cucco basin (0.65 Km^2) saw an extreme event in 2003 that triggered an unusually large debris flow in the area.

In order to test the multi-source, multi-scale and multi-temporal coherence of spatial heterogeneous data, fundamental for assessing the impact of topographic changes, a UAV- based survey of Rio Cucco was conducted by our team in June 2024. The presence of a natural pine forest over much of the basin surface directed us toward the choice of a LiDAR sensor for dense point cloud acquisition and DEM production. After post-processing and analysis of these datasets, a comparison was needed with the same type of data provided by EAGLE FVG (official geo portal of Friuli Venezia Giulia). The aim from this comparison is to document the temporal changes occurring in Rio Cucco and to harmonize different datasets referred to the same study area. To this purpose, the data will be analysed and validated in terms of point clouds density, georeferencing, accuracy, and uncertainties by exploiting data co-registration algorithms. Furthermore, to assure the optimal output for the geomorphometric approach, a land cover classification procedure was tested relying on a simple deep learning model.

2 STUDY AREA

The Rio Cucco basin is a torrential watercourse located in the municipality of Malborghetto-Valbruna (Udine, Italy) where it serves as a right tributary of the Fella River. Its watershed comprises two sub-basins, fed by smaller channels and two main branches that converge into an alluvial fan near the village of Cucco. The basin's geology features dolomites and dolomitic limestones from the Anisian Ladinian period (Dolomia dello Sciliar), along with nodular limestones, marls, and calcarenites in its upper areas. The southern slopes of Monte Cucco are marked by vertical rocky cliffs, frequent rockfalls, and debris accumulations, particularly in regions dominated by friable calcareous and dolomitic rocks prone to thermoclastism and cryoclastism.

The alluvial fan, spanning roughly 0.2 km², hosts a natural pine forest of black pine and Scots pine in its apex and residential areas, meadows, and a state road bridge at its lower end. The predominantly south-facing aspect, combined with arid conditions caused by the area's permeability and frequent material deposition, inhibits soil formation. Annual precipitation averages 1,500 mm, with summer and autumn peaks corresponding to increased debris flow activity. Significant flood events, such as those in June 1996 and August 2003, caused extensive sediment mobilization and damage, with the latter involving 325 mm of rainfall over 12 hours and the transport of approximately 80,000 m³ of sediment.

After the 2003 flood, more than 300 million euros were invested throughout the Valcanale and Canal del Ferro to secure, restore existing hydraulic works as well as build new structures on the most affected basins (FVG Region, 2007). Two branches of the basin were extensively reworked with the construction of cross works and berms, which converge to a downstream storage basin of 100,000 m³. The latter, in particular, is protected by two cyclopean boulder embankments, joined by a filtering weir that conveys the solid-liquid material to a reinforced concrete gutter near the State Road crossing, which is followed by another channelling work in cemented boulders to the point of discharge into the Fella River. The basin plays a vital role in mitigating flood risks, directing sediment-laden flows into reinforced concrete channels towards the Fella River. Figure 1 shows the location of the basin with respect to the surrounding area.
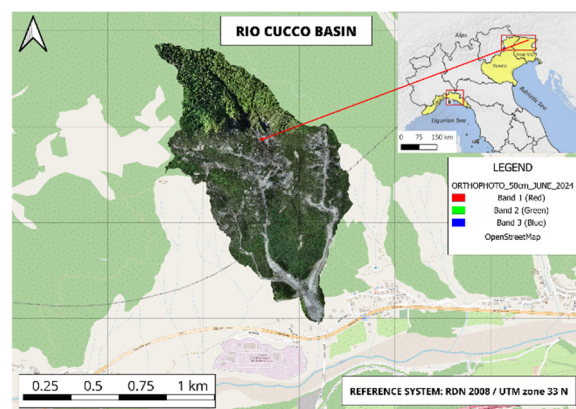

Figure 1: Rio Cucco Basin.

3 METHODOLOGIES

In the case of Rio Cucco, the area was studied by comparing FVG 2017 data with the survey that was conducted in the period between 11 and 14 June 2024.

The EAGLE FVG survey occurred in 2017 thus all the data including the point clouds and digital terrain model refer to that survey. There were two aspects that were considered for the comparison. The point clouds and digital terrain models were used in the main comparison criteria. Moreover, after the comparison between the datasets, a deep learning models was explored to assure the optimal output for the geomorphometric approach, main goal of the MORPHEUS Project.

3.1 Point Clouds

A DJI Matrice 300 RTK drone equipped with a DJI Zenmuse L1 Lidar sensor was used to acquire the point cloud in the June 2024 survey. Consequently, DJI Terra software was used to process the data from the drone and create the point clouds of the area (DJI, n.d.). The point cloud that was output from the software was a merged file that contained all the point clouds of the area surveyed and individual point cloud segments that make up the merged point cloud. Both the merged and the individual point clouds were saved. Table 1 shows the different parameters used in the production of the point clouds with DJI Terra.

The output merged point cloud .las file was 32.6 GB in size which made the file demanding from a computational point of view. Spatial subsampling was used in CloudCompare to reduce the density and size of the point clouds to a workable size (Girardeau-Montaut, n.d.) .

The point clouds were subsampled at spaces of:

- 0.50 (size: 0.4 GB)
- 0.25 (size: 1.9 GB)
- 0.20 (size: 2.3 GB)
- 0.15 (size: 3.8 GB)
- 0.10 (size: 7.1 GB)

Spatial subsampling has an inverse relationship with cloud density. A larger spatial subsampling leads to higher workability but less data. The aim was to find a workable point cloud with a point cloud density greater than 16 points/m^2.

Table 1: DJI Terra Software Parameters.

DJI Terra	
Point Cloud Optimization Parameters	
Point Cloud Density (by Percentage)	High
Point Cloud Effective Distance Range	3 – 300 m
Optimise Point Cloud Accuracy	Yes
Smooth Point Cloud	Yes
Point Cloud Output Parameters	
Ground Point Classification	Yes
Ground Point Classification Parameters	Ground Point Type: Steep Slope Maximum Diagonal of the Building: 25 m Iteration angle: 9° Iteration distance: 0.6 m
DEM Parameters	By GSD ⏐ 0.5 m
Point Cloud Format	PNTS ⏐ LAS
Merged Output	Yes
LiDAR Point Cloud Block Count	9
Output Coordinate System	WGS 84 / UTM zone 33N ⏐ Default

The EAGLE FVG point clouds refer to the acquisition conducted in the area in 2017 and had RDN 2008 UTM 33N as the default reference system. The comparison conducted between the recent data in 2024 and the EAGLE FVG 2017 data was based on two main parameters. The surface density of the point clouds and the Cloud to Cloud distance were used as the comparison parameters of this study taking the same reference system into account.

3.2 Digital Terrain Models

The digital terrain model (DTM) produced using DJI Terra was based on its classification of ground points and non-ground points according to its own algorithm. The parameters used for the creation of the DTM were mentioned in Table 1(regarding the slope steepness, maximum diagonal of the building etc.).

The output DTM was a digital terrain model with removal of canopy and a resolution of 0.5 m as set in the DJI Terra. If no classification of ground points was selected, the result would be a digital surface model that has no separation between ground points and canopy. It is to be noted that the parameters were tweaked to produce the most connected DTM. Keeping the default values they resulted in a heavily tiled DTM that had empty spaces between different tiles. Moreover, the subsampled point cloud with the 0.25 spatial spacing was input into Agisoft Metashape

to produce a DTM with the same resolution of 0.5 m (Agisoft LLC, n.d.).Using Agisoft Metashape to create a digital terrain model from the produced point cloud serves as an alternative to DJI Terra to see how different algorithms behave in digital terrain model generation.

After the comparison between the digital terrain models produced using DJI Terra & Agisoft Metashape, the next step was comparing the digital terrain models to EAGLE FVG digital terrain models for the year 2017. The files on the EAGLE FVG website were in ascii format and yielded several tiles that were merged and clipped to the shape of the Rio Cucco basin. As previously conducted with the comparison of the point clouds, the 2024 DTM was converted to the reference system of the EAGLE FVG 2017 DTM (RDN 2008 UTM 33N) to create a Difference of Digital Elevation between the two digital terrain models.

3.3 Land Cover Classification Using a Deep Learning Model

An important task for this project is conducting land cover classification of the Rio Cucco basin so that land cover and land use can be quantified and monitored for the area. Land cover classification is particularly useful to monitor natural hazards. There have been studies regarding the usage of land cover classification in risk management. UAV very high resolution data was used in the classification of the Niger River (Belcore et al., 2022). The authors used a multitude of geomatic techniques to process the data and enrich feature extraction based on spectral, textural and elevation data acquired from the survey. This allowed for the creation of different classes necessary for the food map creation to an area that had very little coverage. Covering another work by these authors, mountainous areas in Italy studied in land cover classification using Google Earth Engine. That study addressed the challenges of accurately classifying mountainous areas due to the variability of reflectance and shadows (Belcore et al., 2020). A land cover classification is required for Rio Cucco and as a requirement of the project MORPHEUS, artificial intelligence techniques need to be explored for automatic classification of the study area. Deep learning, specifically through the use of convolutional neural networks (CNNs), offers a powerful approach to semantic segmentation of satellite imagery (Zhang et al., 2019). This involves classifying each pixel in an image into a specific category or class (e.g., building, road, forest). Consequently, an open-source semantic segmentation model was used to conserve

time as well as explore the feasibility of deep learning applications for this work.. The model DeepLabV3 ResNet50 model was developed as an open-source library on Python. As this model is not particularly only made for satellite images and remote sensing, the model needed training. The model was trained with a Kaggle dataset of satellite images that contains the images alongside their masks (Kaggle, n.d.). This dataset itself is compiled from three main datasets labeled: Semantic segmentation of aerial imagery (Roia Foundation), Land Cover Classification - Bhuvan Satellite Data (Indian Space Research Organization) , Urban Segmentation (International Society for Photogrammetry and Remote Sensing). The dataset contained classes shown in Table 2. These classes were used as they are and in their same color in the training and testing of the data to see the effectiveness of the model.

Table 2: Dataset Default Classes.

Class	Color
Building	Dark Purple
Land / Unpaved area	Light Purple
Road	Light Blue
Vegetation	Yellow
Water	Orange
Unlabeled	Gray

Table 3 summarizes the different parameters used in the deep learning model training.

Table 3: Deep Learning Model Parameters

Parameter	Value	Description
Batch Size	8	Number of images processed in parallel during training
Image Dimensions	256 x 256	Resized dimensions of input images
Number of Classes	6	Number of distinct classes
Model Architecture	DeepLabV3 (ResNet50)	The backbone used for feature extraction and segmentation
Pretrained Weights	COCO_WITH_VOC_LABELS_V1	Weights pretrained on the COCO dataset
Dataset Size	203 images	Total number of image-mask pairs
Training Epochs	400 epochs	Total number of epochs used in training
Input Channels	3 (RGB)	Number of channels in the input image
Output Channels	6	Number of segmentation classes predicted by the model

After training the model with that dataset for more than 400 iterations, a new orthophoto was input to test the model. The orthophoto for the area was compiled by converting the subsampled 0.25 point cloud in Agisoft Metashape into create an orthophoto. With respect to the 2017 orthophoto, the data was downloaded from EAGLE FVG. Both datasets were resampled to be 0.5 m in resolution. The main objective of these orthophotos was to create testing for the deep learning model being developed for this project.

4 RESULTS

Comparing the different datasets for Rio Cucco, it is evident that were changes in the area from 2017 to 2024.The changes were particularly evident when the difference of digital elevation (DoD) was calculated. There were areas where there was possible sediment deposition leading to an elevation increase at the location of the deposition and an elevation decrease where the sediments disconnected. This indicates that a rockfall possibly occurred between 2017 and 2024.

4.1 Point Clouds

4.1.1 Surface Density

Based on several iterations to choose the best subsample with respect to its usability and its resolution. It was found that the 0.15 spatial subsample model was the most preferable serving a high ratio between resolution and workability. This point cloud had more than 95 % of its density greater than 16 points/m^2 but it was light enough to run without causing any issues. Since the point clouds produced during the June 2024 survey were larger than the basin. The selected point cloud would be then trimmed based on the boundaries of the basin and used to directly compare with the EAGLE FVG 2017 points cloud based on the same area of interest in the basin.

Table 4: Surface Density of Rio Cucco Point Cloud Subsamples 2024.

Surface Density (points/m^2)					
Pt Cloud	μ	σ	Min	Max	% of pts > 16 pts/m^2
0.5	10.8	6.1	0.32	21.2	25.0
0.25	54.9	31.6	0.32	109.4	85.6
0.2	94.2	54.4	0.32	188.0	91.4
0.15	171.9	99.4	0.32	343.4	95.3
0.1	390.3	226.0	0.32	780.3	97.7

Based on the results from Table 5, both point clouds show very similar surface density with both having more than 95 % of their points being significantly higher than the required 16 points/m^2.

Table 5: Surface Density of Clipped Rio Cucco Point Cloud FVG 2017 and 0.15 Subsample 2024.

Surface Density (points/m^2)					
Pt Cloud	μ	σ	Min	Max	% of pts > 16 pts/m^2
2017	190.1	110.0	0.32	379.9	95.7
2024	171.4	99.2	0.32	342.4	95.3

4.1.2 Cloud to Cloud Distance

Next, to accurately check the differences between the point cloud of 2017 and the one created in June 2024, the boundaries between both point clouds should be identical and the reference system should also be identical. The reference system that should be worked on is RDN2008 UTM 33N, which is the same reference system used by EAGLE FVG.

Furthermore, the Cloud-to-Cloud distance was performed before and after ICP by placing the EAGLE FVG point cloud as the reference option and the Rio Cucco 2024 0.15 Subsample point cloud as the compared option in each scenario. The Cloud to Cloud Distance helps in identifying what the differences between both point clouds were during the different time periods of the area.

Table 6 shows the differences in the Cloud to Cloud distance between the same point clouds from June 2024 saved in different formats and the 2017 EAGLE FVG point cloud.

Table 6: Cloud to Cloud Distance Between the 2017 EAGLE FVG Point Clouds and 0.15 Subsample 2024.

Cloud 2 Cloud Distance (m)					
Pt Cloud	μ	σ	Min	Max	% of pts < 1m
Before ICP					
RDN	3.7	2.1	0.00	7.4	13.7
After ICP (85 % Final Overlap)					
RDN	3.6	2.1	0.00	7.2	14.1

As seen from Table 6, performing an ICP slightly reduces the nearest neighbor distance between the two point clouds. Observing that table, it is possible to notice a decrease in the mean distance of about 10 cm with the same standard deviation, which means that both EAGLE FVG data and the authors data are been produced with the same accuracy in georeferencing. It is noticeable that the mean distance between the point clouds is more than three meters.

This would be better explained in the next section when the difference of digital elevation is calculated.

4.2 Digital Terrain Models

Regarding the comparisons between the DJI Terra DTM, the Agisoft Metashape DTM, and the EAGLE FVG, the analysis showed that it was favourable to use the DJI Terra DTM to compare with the EAGLE FVG DTM. Regarding the comparisons between the DJI Terra DTM, the Agisoft Metashape DTM, and the EAGLE FVG, the analysis showed that it was favourable to use the DJI Terra DTM to compare with the EAGLE FVG DTM. This was due to having little difference between the Agisoft Metashape and DJI Terra DTM, but the Agisoft Metashape DTM interpolated areas that were not acquired in the point cloud. Also, the DJI Terra DTM had an advantage of containing the data from all the points instead of a subsampled point cloud.

Consequently, a Difference of Digital Elevation (DoD) was performed between the DJI Terra DTM of the year 2024 and the EAGLE FVG DTM of the year 2017.
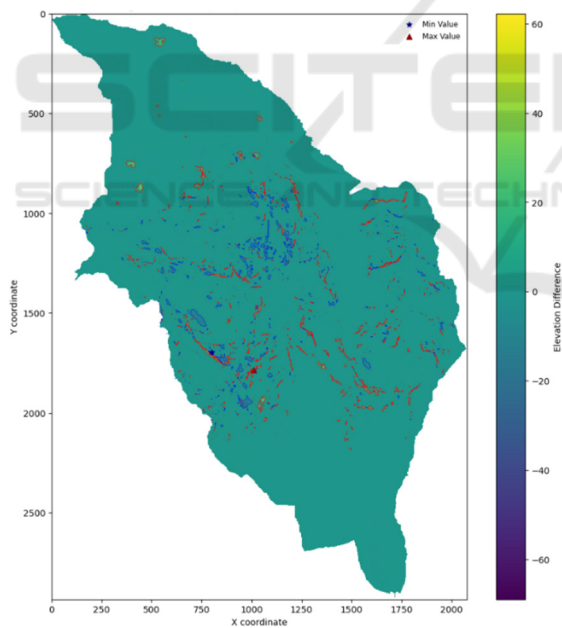

Figure 2: Difference of Digital Elevation (DoD) Between DJI Terra 2024 and EAGLE FVG 2017 DTMs.

Clearly, there were differences between the two digital terrain models particularly highlighted in the pinnacles of the terrain and tops of the rocks in that inclined area. When highlighting the $\mu + 3\sigma$ and $\mu - 3\sigma$ areas we see that areas contoured in blue show an elevation decrease whereas areas with a red contour

signify an elevation increase. The areas that remained in teal blue and showed no contour experienced minimal change. Rockfall can be tied to the high difference between 2024 and 2017. Based on figure, the areas that lost elevation ended up depositing the elevation lower in the basin which is typical of rockfall situations. There were some areas shown in yellow that were trees not cleaned properly with the DJI Terra software and was considered as ground points while clearly, they were not.

4.3 Land Cover Classification Using a Deep Learning Model

Upon completion of the model training, the model began to recognize patterns and identify the classes found in the control images based on their classified masks. After this step, the Rio Cucco orthophotos were introduced. Both datasets which refer to the Rio Cucco 2024 orthophoto and the Rio Cucco 2017 orthophoto were tested to check the effectiveness of the model at identifying the classes in an unintroduced image. The semantic segmentation with this deep learning model in its current form produced mixed results in terms of its classification as it detects vegetation, and bare land well but struggles with accurately detecting roads and buildings in the new image. Based on Figure 3, it is evident that the model works very well at predicting the classes based on the images that it has gotten used to (its original dataset). In Figure 4 however, it can be observed that the model recognizes the shapes and is able to detect well the land (represented in light purple) while mistaking vegetation as water (orange instead of purple). The model produced mixed results with buildings as it was able to recognize their location but did not have proper edge detection for them. The testing of this model yielded mixed results in terms of its segmentation abilities.
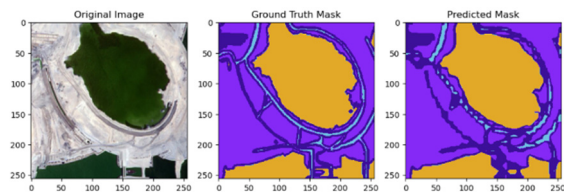
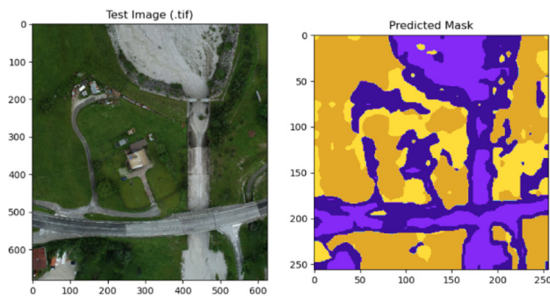

Figure 3: Deep Learning Model Training Results.

Figure 4: Deep Learning Model Results with Rio Cucco Orthophoto.

Figure 5: Rockfall in Sloped Areas in Rio Cucco (2024).

5 DISCUSSIONS

With respect to the Rio Cucco basin, comparing past data with present data is quintessential to understand the differences both spatially and temporally. Based on the findings of the data when comparing the data of the survey in 2024 and the FVG 2017 data taken from EAGLE FVG, the differences that existed were evident especially when conducting the DoD. The DoD pointed to an increase of elevation in certain areas and a decrease in elevation in others. The increase of elevation was found further down the slope and the decrease of elevation was found higher in the slopes. Several explanations could be tied to why this variation of elevation occurred. The variation could have been tied to possible rockfall events that happened and lead to sediment deposition by removing debris from higher up the slope to be deposited further down the slope. However, the variations could have also been due to errors in the model itself. To clarify which case most likely caused this variation between the two DTM, an examination of the drone images for the June 2024 survey was done. After careful examination, rock debris was noticed downstream in the areas consistent with the blue and red colour contours. Fig.5 shows an image of rocks deposited near a slopped area in the basin. Based on the location of the rock deposition, it can be inferred that the elevation differences in the DTM were most likely due to a rockfall event.

Based on the history of the area and the nature of its geology, it is expected that rockfall events will continue to occur in the area especially because of the calcareous and dolomitic set of rocks that are subject to thermoclastism and cryoclastism. With respect to the deep learning model, the testing showed mixed results in terms of its power at classifying unintroduced images. Other steps to increase the effectiveness of the model would include data augmentation techniques and introducing the digital terrain models or the digital surface models in the training phase so that the model can segment the area with respect to certain elevation patterns differentiating between water, road, buildings, vegetation and other classes.

6 CONCLUSIONS

In summary, the Rio Cucco basin is subject to several changes over the years and needs to be monitored in terms of natural hazard studies. The geological parameters as well as the morphology makes the Rio Cucco basin particularly liable to the effects of climate change. The nature of its rock formations and slopes which are prone to weathering due to abrupt changes in temperature highlights the importance of consistent monitoring. With the advancement of geomatic techniques , artificial intelligence (AI) models, and internet of things (IoT) sensors, perhaps a predictive approach could be pursued to model where and when natural hazards in the area would most likely occur. Consequently, preventative measures could be taken to reduce the impact of these events that are likely to become more common with the emergence of climate change.

ACKNOWLEDGEMENTS

REFERENCES

Agisoft LLC. (n.d.). *Agisoft Metashape*. https://www.agisoft.com

Belcore, E., Piras, M., & Pezzoli, A. (2022). Land Cover Classification from Very High-Resolution UAS Data for Flood Risk Mapping. *Sensors*, *22*(15), 5622. https://doi.org/10.3390/s22155622

Belcore, E., Piras, M., & Wozniak, E. (2020). Specific Alpine Environment Land Cover Classification Methodology: Google Earth Engine Processing for Sentinel-2 Data. *The International Archives of the Photogrammetry, Remote Sensing and Spatial Information Sciences*, *XLIII-B3-2020*, 663–670. https://doi.org/10.5194/isprs-archives-XLIII-B3-2020-663-2020

Cavalli, M., Trevisani, S., Comiti, F., & Marchi, L. (2013). Geomorphometric assessment of spatial sediment connectivity in small Alpine catchments. *Geomorphology*, *188*, 31–41. https://doi.org/10.1016/j.geomorph.2012.05.007

DJI. (n.d.). *DJI Terra - Make the World Your Digital Asset - DJI*. https://enterprise.dji.com/it/dji-terra

Girardeau-Montaut, D. (n.d.). *CloudCompare - Open Source project*. https://www.danielgm.net/cc/

Huggel, C., Clague, J. J., & Korup, O. (2012). Is climate change responsible for changing landslide activity in high mountains? *Earth Surface Processes and Landforms*, *37*(1), 77–91. https://doi.org/10.1002/esp.2223

Indian Space Research Organization. (2023, May 31). *Land cover Classification : Bhuvan Satellite Data*. Kaggle. https://www.kaggle.com/datasets/khushiipatni/satellite-image-and-mask

International Society for Photogrammetry and Remote Sensing. (2024, March 20). *Urban Segmentation - ISPRS*. Kaggle. https://www.kaggle.com/datasets/aletbm/urban-segmentation-isprs

Kaggle. (n.d.). *Kaggle: your machine learning and data science community*. https://www.kaggle.com/

Roia Foundation. (2020, May 29). *Semantic segmentation of aerial imagery*. Kaggle. https://www.kaggle.com/datasets/humansintheloop/semantic-segmentation-of-aerial-imagery

Sangelantoni, L., Gioia, E., & Marincioni, F. (2018). Impact of climate change on landslides frequency: The Esino river basin case study (Central Italy). *Natural Hazards*, *93*(2), 849–884. https://doi.org/10.1007/s11069-018-3328-6

Schneiderbauer, S., Fontanella Pisa, P., Delves, J. L., Pedoth, L., Rufat, S., Erschbamer, M., Thaler, T., Carnelli, F., & Granados-Chahin, S. (2021). Risk perception of climate change and natural hazards in global mountain regions: A critical review. *Science of The Total Environment*, *784*, 146957. https://doi.org/10.1016/j.scitotenv.2021.146957

Semnani, S. J., Han, Y., Bonfils, C. J., & White, J. A. (2025). Assessing the impact of climate change on rainfall-triggered landslides: A case study in California. *Landslides*. https://doi.org/10.1007/s10346-024-02428-0

Zhang, C., Sargent, I., Pan, X., Li, H., Gardiner, A., Hare, J., & Atkinson, P. M. (2019). Joint Deep Learning for land cover and land use classification. *Remote Sensing of Environment*, *221*, 173–187. https://doi.org/10.1016/j.rse.2018.11.014